processes

MDPI

Article

Development of Environmental Friendly Dust Suppressant Based on the Modification of Soybean Protein Isolate

Hu Jin [1,2], Wen Nie [1,2,3,*], Yansong Zhang [1,2], Hongkun Wang [2], Haihan Zhang [2], Qiu Bao [2] and Jiayi Yan [2]

1 Key Laboratory of Ministry of Education for Mine Disaster Prevention and Control, College of Mining and Safety Engineering, Shandong University of Science and Technology, Qingdao 266590, China; 15764250719@163.com (H.J.); hk19941211@163.com (Y.Z.)

2 College of Mining and Safety Engineering, Shandong University of Science and Technology, Qingdao 266590, China; SKDWHK@163.com (H.W.); 15065423187@163.com (H.Z.); m15610569565@163.com (Q.B.); yan18739937718@163.com (J.Y.)

3 Hebei State Key Laboratory of Mine Disaster Prevention, North China Institute of Science and Technology, Beijing 101601, China

* Correspondence: niewen@sdust.edu.cn; Tel.: +86-189-5483-5917

Received: 25 February 2019; Accepted: 15 March 2019; Published: 20 March 2019

Abstract: Aiming to further improve the dust suppression performance of the dust suppressant, the present study independently develops a new type of biodegradable environmentally-friendly dust suppressant. Specifically, the naturally occurring biodegradable soybean protein isolate (SPI) is selected as the main material, which is subject to an anionic surfactant, i.e., sodium dodecyl sulfonate (SDS) for modification with the presence of additives including carboxymethylcellulose sodium and methanesiliconic acid sodium. As a result, the SDS-SPI cementing dust suppressant is produced. The present study experimentally tests solutions with eight different dust suppressant concentrations under the same experimental condition, so as to evaluate their dust suppression performances. Key metrics considered include water retention capability, cementing power and dust suppression efficiency. The optimal concentration of dust suppressant solution is determined by collectively comparing these metrics. The experiments indicate that the optimal dust suppressant concentration is 3%, at which level the newly developed environmentally-friendly dust suppressant solution exhibits a decent dust suppression characteristic, with the water retention power reaching its peak level, and the corresponding viscosity being 12.96 mPa·s. This performance can generally meet the requirements imposed by coal mines. The peak efficiency of dust suppression can reach 92.13%. Fourier transform infrared spectroscopy (FTIR) and scanning electron microscopy (SEM) were used to analyze the dust suppression mechanism of the developed dust suppressant. It was observed that a dense hardened shell formed on the surface of the pulverized coal particles sprayed with the dust suppressant. There is strong cementation between coal dust particles, and the cementation effect is better. This can effectively inhibit the re-entrainment of coal dust and reduce environmental pollution.

Keywords: soybean protein isolate modification; dust suppressant; performance characterization; optimal concentration; analysis of dust suppression mechanism

1. Introduction

Coal serves as the fundamental source of energy in China. Throughout the foreseeable future, coal will still occupy a significant proportion of primary energy in China [1–5]. During the outdoor storage of coal piles and railroad transportation of coal, a large amount of coal dust may be generated,

which not only causes the loss of coal and waste of natural resources, but also leads to severe environmental pollution [6–12]. Besides, as for coal piles, the dust dispersion can adversely impact the normal operation of electric and mechanical equipment as well as the monitoring system, leading to a shortened lifespan. More seriously, the increase of dust concentration can pose a major threat to operational safety, triggering the occurrence of accidents [13–17]. The traditional dust suppression methods include water spray and tarp coverage, which are unfavorable due to high cost and poor long-term dust suppression performance. Therefore, scholars in the international community have started to develop chemical-based dust suppression methods, which have proven to be promising in many dust suppression applications [18–24]. Overall, the chemical dust suppressant is highly favored considering its dust suppression effect, economic viability and environmental-friendliness, and therefore has a vast potential for future development [25–30]. The chemical dust suppressant functions effectively on open dust sources, and therefore this technology has been widely applied to those enterprises with a major generation of coal dust, such as railroad transportation departments, dumping sites and thermal power plants [31–36]. In recent years, the domestic and foreign research on chemical dust suppressant is shifting its focus to enhancing recyclability, environmental-friendliness, and efficiency [37–42]. Bao et al. [43] took corn starch as the main raw material and developed a kind of super absorbent dust suppressant by chemical modification method, which can effectively inhibit the dust diffusion during coal transportation. Grogan [44] conducts research on combining the byproduct of biodiesel production, i.e., glycerol, with surfactant, polyhydroxy esters and acrylic acid compound to produce a dust suppressant, with its performance being characterized. The prepared suppressant has a decent dust suppression effect and is environmentally friendly. Zhang et al. [45] employs glasswort as the raw material, which is blended with sodium dodecylbenzene sulfonate and carboxylmethyl cellulose as the additives to produce an ecologically friendly dust suppressant. Zhang et al. [46] prepared a degradable dust suppressant by chemical modification using a polymer material guar gum as the main raw material. The dust suppressant has good wettability and water retention. Yang et al. [47] utilizes film coalescing aid, fatty alcohol polyoxyethylene ether and polyvinyl alcohol as the raw materials to develop a dust suppressant with a decent ability to withstand rainfall and wind, making it primarily applied to coal transportation. The spray of this suppressant causes a thick hardened layer to form on the particles surface, resulting in a long dust suppression duration. Polat H. et al. [48] uses Polyethylene oxide (PEO)/PO as the raw material to synthesize a dust suppressant, which can effectively wet the coal dust during the mining process while mitigating the equipment corrosion.

The application of cementing dust suppressant is an effective method for preventing and controlling dust dispersion, with cementing power, water retention ability and dust reduction efficiency being the key factors dictating the dust suppression performance of the cementing dust suppressant. Although those aspects have been extensively discussed by domestic and overseas scholars, their studies are mainly focused on certain individual characteristics, without covering the entire suite of metrics [49–53]; also, those cementing dust suppressants are subject to certain disadvantages, including toxicity, lack of biodegradability, and the tendency to cause secondary pollution, etc. [54–60]. To address the aforementioned problems, the present study uses biodegradable and environmentally-friendly soybean protein isolate (SPI) as the main material. SPI is a main ingredient of soybean. It contains a large amount of active functional groups, and is favored for its biodegradability, and available from various resources. It is therefore an environmentally-friendly material for producing environmentally-friendly and pollution-free dust suppressant [61–69]. The present study uses sodium dodecyl sulfonate to modify the SPI while adding carboxymethylcellulose sodium and methanesiliconic acid sodium to the mixture so as to develop a new type of environmentally-friendly naturally-occurring macromolecular dust suppressant, namely SDS-SPI cementing dust suppressant; subsequently, the present study experimentally measures a suite of performance metrics associated with the newly developed dust suppressant, based on which the

optimal dust suppressant concentration is determined. At the same time, the research results also provide ideas for the development of other types of high-efficiency environmental dust suppressants.

2. Experiments

2.1. Main Equipment and Raw Materials

The reagents and equipment used in the present study are listed in Tables 1 and 2.

Table 1. Primary raw materials used in the experiment.

Chemical Name	Chemical Formula	Purity	Manufacturer
Soybean protein isolate	$C_{13}H_{10}N_2$	BR	Sinopharm Chemical Reagent Co., Ltd., Beijing, China
Carboxymethylcellulose sodium	$C_8H_{11}O_7Na$	CP	Xiya Reagent Co., Ltd., Chengdu, China
Methanesiliconic acid sodium	CH_5SiO_3Na	CP	Shandong Yousuo Chemical Technology Co., Ltd., Qingdao, China
Sodium dodecyl sulfonate	$C_{12}H_{25}OSO_3Na$	Tech	Shandong Yousuo Chemical Technology Co., Ltd., Qingdao, China

Notes: BR indicates that the chemical reagent is a biochemical reagent; CP indicates chemical purity; Tech indicates an industrial reagent.

Table 2. Key experimental equipment and specifications.

Experimental Equipment	Specifications	Manufacturer
Rotary viscometer	NDI-79	Shanghai Precision Instrument Co., Ltd. Shanghai, China
High-Resolution Scanning Electron Microscope	Nova Nano SEM	Shanghai Casting Gold Analytical Instruments and Equipment Co., Ltd. Shanghai, China
Fourier-transform infrared spectroscope	Nicolet (iS10)	Beijing Kaifeng Fengyuan Technology Co., Ltd. Beijing, China
Coal mine dust sampler	AKFC-92	Qingdao Lubo Weiye Environmental Protection Technology Co., Ltd. Qingdao, China
Mine energy-saving axialfan	ASZ-11.2	Zibo Jinhe Fan Co., Ltd. Zibo, China

2.2. Preparation of SDS-SPI Cementing Dust Suppressant

Put 7.50 g of SPI (Sinopharm Chemical Reagent Co., Ltd., Beijing, China), 0.15 g of sodium dodecyl sulfonate (SDS, Shandong Yousuo Chemical Technology Co., Ltd., Qingdao, China), 0.15 g of carboxymethylcellulose sodium (CMC, Xiya Reagent Co., Ltd., Chengdu, China) and 140 mL of water in a three-neck round-bottom flask with sufficient stirring. Raise the temperature of the solution to 60 °C and let the reaction last for one hour at this temperature. Then let the solution cools down. 2.50 g of 30% methanesiliconic acid sodium was added to the solution, followed by stirring it evenly. The experiment finally developed a SDS-SPI cementing dust suppressant with a soy protein isolate concentration of 5%. The stirring speed is controlled to be 60–80 r/min throughout the reaction process to prevent the solution from foaming in a large amount. In the process of application, the dust suppressant solution was diluted by different multiples, resulting in modified SDS-SPI cementing dust suppressant solutions whose SPI concentrations are 1%, 1.5%, 2%, 2.5%, 3%, 3.5%, 4% and 5%, respectively.

2.3. Application of SDS-SPI Cementing Dust Suppressant

The coal samples used in the experiment were coking coal from the 20,206 fully mechanized working face of Zaozhuang Corporation's Jiangzhuang, Shandong province. Coal samples were ground into pulverized coal using a planetary motion micro mill, and then fine pulverized coal with particle size less than 3 mm was screened through a sieve with a hole size of 3 mm. The prepared coal

sample is dried in a vacuum drying chamber (Shanghai lang gan experimental equipment co., LTD, Shanghai, China) at a temperature of 100 °C. The fine coal particles with a particle size of 0–3 mm was placed in 9 Petri dishes. The extrusion method was used to flatten the surface of the sample and then eight kinds of dust suppressant solutions with different SPI concentrations were evenly sprayed onto the corresponding eight coal samples with a density of 2 L/m^2. The ninth coal sample was evenly sprayed with water.

3. Characterization of Properties

3.1. Experimental Characterization of Water Retention Performance of Dust Suppressant

The water retention of a dust suppressant can be measured through its ability to resist evaporation. Under the same experimental condition, an improved water retention of dust suppressant corresponds to an enhanced anti-evaporation characteristic, leading to an improved dust suppression effect. The anti-evaporation characteristic of a solution can be measured with the evaporation rate, where a low evaporation rate indicates a good anti-evaporation performance. Therefore, the present experiment characterizes the dust suppressant's water retention based on measuring the evaporation rate. The experimental procedure is outlined below: under the same experimental condition, put the desiccated coal sample in a labeled clean Petri dishes; evenly spray the prepared SDS-SPI cementing dust suppressant solutions at different concentrations over the surface of coal sample at 2 L/m^2. Weigh the sample after its absorption of solution reaches a sufficient level. Then put the sample in a vacuum drying chamber and keep the temperature at 60 °C (Figure 1). At a set interval, take the sample out of the oven and weigh its mass; the evaporation rate can thereby be calculated with Equation (1). The final results, as shown in Table 3, can be obtained by linear fitting between measurement results and time. The corresponding fitted curves are shown in Figures 2 and 3.

$$\theta = \frac{W_1 - W_2}{A\ T} \tag{1}$$

where θ denotes the where evaporation rate of dust suppressant (g·m^{-2}·s^{-1}); W_1 denotes the coal sample mass before evaporation (g); W_2 denotes the coal sample mass post evaporation (g); A denotes the evaporation area of coal sample (m^2); and T denotes the evaporation time (s).

Figure 1. Vacuum drying chamber with a preset temperature.

Table 3. Evaporation rate of dust suppressant ($g \cdot m^{-2} \cdot s^{-1}$).

Sample (%)	Time (h)											
	0.5	**1**	**1.5**	**2**	**2.5**	**3**	**4**	**5**	**6**	**8**	**10**	**12**
water	0.062	0.055	0.051	0.042	0.038	0.023	0.015	0.012	0.008	0.008	0.005	0.005
1	0.058	0.052	0.047	0.039	0.035	0.021	0.013	0.013	0.008	0.007	0.003	0.003
1.5	0.045	0.042	0.036	0.034	0.028	0.021	0.012	0.009	0.009	0.007	0.007	0.004
2	0.043	0.040	0.035	0.031	0.025	0.019	0.011	0.008	0.008	0.006	0.006	0.004
2.5	0.031	0.029	0.023	0.017	0.015	0.015	0.010	0.005	0.005	0.003	0.003	0.002
3	0.030	0.028	0.023	0.016	0.012	0.010	0.009	0.006	0.004	0.004	0.002	0.002
3.5	0.034	0.030	0.025	0.018	0.013	0.013	0.011	0.008	0.007	0.004	0.004	0.003
4	0.042	0.038	0.034	0.029	0.024	0.014	0.010	0.009	0.008	0.008	0.005	0.005
5	0.048	0.043	0.035	0.026	0.022	0.018	0.014	0.011	0.010	0.009	0.006	0.006

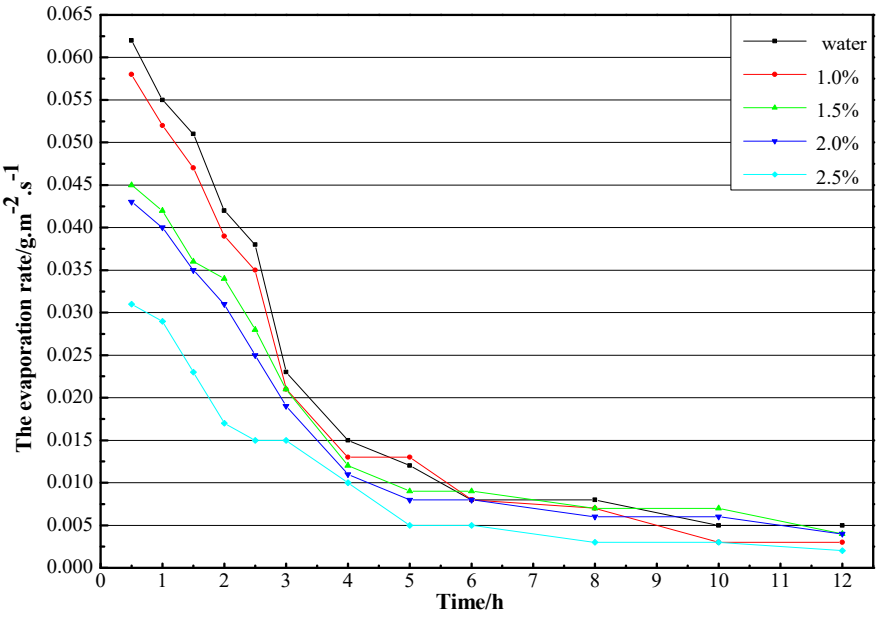

Figure 2. Trend chart of sample evaporation rate with time (concentration 0%, 1%, 1.5%, 2%, 2.5%).

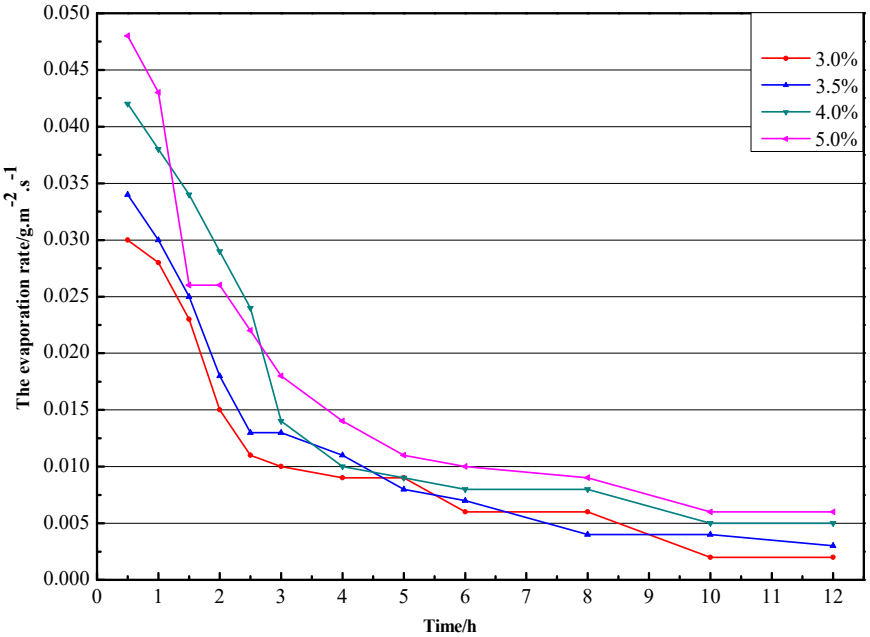

Figure 3. Trend chart of sample evaporation rate with time (concentration 3%, 3.5%, 4%, 5%).

It can be seen in Table 3, Figures 2 and 3 that at the same time and under the same experimental condition, the evaporation rate of clean water is the highest, followed by the evaporation rate of 1% dust suppressant solution. The water evaporation rates of dust suppressant solutions with concentrations between 2.5% and 3.5% are relatively small. It can be inferred from Figures 2 and 3 that the 2.5% and 3% dust suppressant solutions exhibit the smallest evaporation rate, and their evaporation rate curves are relatively flat, corresponding to limited variation of the evaporation amount within the same time window; a further comparison indicates that compared to 2.5% dust suppressant, the 3% dust suppressant solution has the lowest evaporation rate, and its curve does not undergo any major change, implying that its anti-evaporation characteristic, water retention ability and dust suppression effect are the best.

3.2. Viscosity Testing Experiments

The viscosity of coal dust suppressant is a key technical indicator associated with the applicability of samples. This experiment used an NDJ-79 rotational viscometer (Shanghai Precision Instrument Co., Ltd., Shanghai, China) with its rotating shaft suspended from the equipment. Add a 50 mL fluid sample to the test vessel and insert the spindle into the liquid until the level mark on the top of the spindle is immersed in the water. Then adjust the speed knob to keep the speed at 75 rpm. Based on this condition, the viscosity of the prepared SDS-SPI cement dust suppressant solution diluted to various concentrations was measured under the same conditions. The measurement is repeated for three times for each sample, with the mean value treated as the final viscosity of the sample. The measurement results are shown in Table 4; meanwhile, prepare a solution containing SPI only, and measure its viscosity under the same experimental condition, with the measurement results shown in Table 5; finally, one can compare the measurement results derived from two groups, as illustrated in Figure 4, where (A) denotes the viscosity of SPI solution at various concentrations, and (B) denotes the viscosity of modified SDS-SPI cementing dust suppressant solutions at various concentrations.

Table 4. Viscosities of sodium dodecyl sulfonate-soybean protein isolate (SDS-SPI) cementing dust suppressant solutions.

Number	Concentration							
	1%	**1.5%**	**2%**	**2.5%**	**3%**	**3.5%**	**4%**	**5%**
1#	3.68	6.20	10.20	13.28	16.20	19.40	22.48	21.84
2#	3.48	6.76	10.72	12.84	16.76	20.84	21.80	22.72
3#	3.04	7.20	9.56	12.76	16.60	20.72	20.64	22.88
Average Viscosity (mPa·s)	**3.40**	**6.72**	**10.16**	**12.96**	**16.52**	**20.32**	**21.64**	**22.48**

Table 5. Viscosities of SPI solutions.

Number	Concentration							
	1%	**1.5%**	**2%**	**2.5%**	**3%**	**3.5%**	**4%**	**5%**
1#	1.80	3.40	5.01	6.32	8.52	10.29	11.36	12.21
2#	1.92	3.48	5.27	6.59	8.31	10.35	11.44	12.38
3#	1.64	3.32	5.08	7.01	8.61	10.44	11.64	12.61
Average Viscosity (mPa·s)	**1.80**	**3.40**	**5.12**	**6.64**	**8.48**	**10.36**	**11.48**	**12.40**

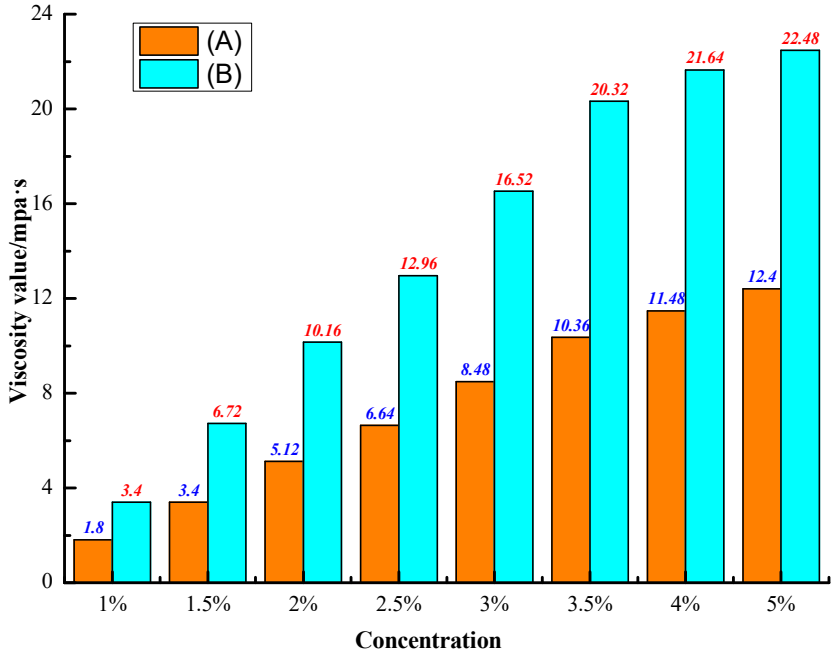

Figure 4. Viscosity histogram.

Figure 4 shows that the viscosity of modified SDS-SPI cementing dust suppressant solution increases rapidly with SPI concentration. The viscosity value is increased substantially compared to the viscosity of the solution with SPI only; as the concentration of SPI in the solution reaches 1.0%, the viscosity of dust suppressant solutions 3.40 mPa·s; as the solution concentration reaches 2.5%, the viscosity of the solution with SPI is merely 6.64 mPa·s, whereas the viscosity of the modified dust suppressant solution has reached 12.96 mPa·s, which is more than twice that of pure SPI solution. Therefore, the dust suppression effect of SDS-SPI cementing dust suppressant solution is more pronounced. As for the dust suppressant solution used in coal mines, considering the economic cost and the dust suppression effect, it would be non-ideal to have an excessively high viscosity. Usually the range of viscosity lies between 12.0–20.0 mPa·s. For this reason, the SDS-SPI cementing dust suppressant solution with concentration above 2.5% can meet the requirement posed by coal mines.

3.3. Measurement of Dust Suppression Efficiency

The dust suppression efficiency can be employed as a direct metric to indicate the dust suppression effect of a dust suppressant. The present experiment is carried out based on the air tunnel simulation platform located at the Dust Control Laboratory of Shandong University of Science and Technology, as shown in Figure 5. The air tunnel simulation platform consists of aTDI8000-0750G-4T Infinitely Variable Inverter (Yueqing Taida Electrical Technology Co., Ltd., Wenzhou, China) and aSZ-11.2 Axial Fan (Zibo Jinhe Fan Co., Ltd., Zibo, China) (as shown in Figure 6), both of which are made in China. Under the regulation of the inverter, the axial fan can mimic natural wind, whose peak velocity can reach 32 m/s. Place the sample with hardened shell on the platform, and keep the air speed at the sample location at 14~16 m/s. Collect samples, i.e., particles suspended in the air with sizes less than 100 μm, with a coal mine dust sampler (as shown in Figure 7) at the location 3.0 m downstream of the sample. The sampling process is conducted in a continuous mode, with flow rate maintained at 20 L/min. The sampling duration is 30 min. Firstly, one needs to test the air in the experimental chamber for measuring the background concentration; subsequently, the coal sample sprayed with clear water is tested, with the corresponding coal dust concentration measured; as the next step, coal samples treated with dust suppressants of eight different concentrations are tested in a sequential manner, with the corresponding coal dust concentrations in the air recorded. During

the post-processing stage, the dust suppression efficiency of each test can be calculated according to Equation (2). Figure 8 illustrates the testing results.

$$\rho = \left(1 - \frac{\theta_x - \theta_0}{\theta_1 - \theta_0}\right) \times 100\% \quad (2)$$

where ρ denote the dust suppression efficiency (%); θ_0 denote the background dust concentration inside experimental chamber (mg/L); θ_1 denote the dust concentration for coal sample with clear water treatment (mg/L); and θ_x denote the dust concentrations for coal samples treated with different dust suppressants (mg/L).

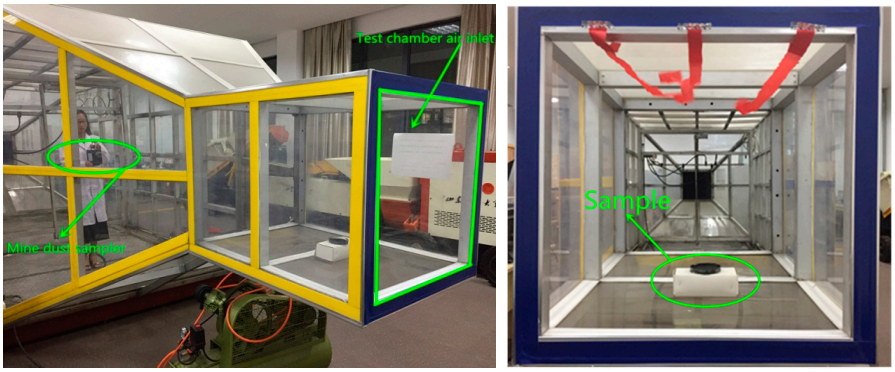

Figure 5. Air tunnel simulation apparatus.

Figure 6. SZ-11.2axial fan.

Figure 7. Coal mine dust sampler.

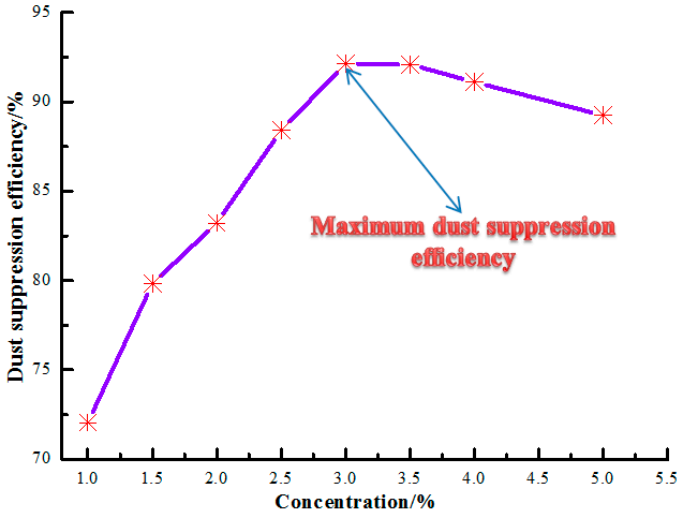

Figure 8. Dust suppression efficiency of sodium dodecyl sulfonate-soybean protein isolate (SDS-SPI) cementing dust suppressants.

Figure 8 shows that as the solution concentration of SDS-SPI cementing dust suppressant increases, the dust suppression efficiency climbs rapidly. As the mass concentration reaches 3.0%, the suppressant's dust suppression efficiency on coal dust peaks at 92.13%; subsequently, the dust suppression efficiency starts to drop, which is primarily due to the fact that an increase of viscosity causes the surface tension of SDS-SPI cementing dust suppressant solution on coal dust surface to increase, leading to a subdued wettability with respect to the coal dust. This change compromises the dust suppression efficiency.

In summary, as the mass concentration of SDS-SPI cementing dust suppressant solution stays at 3.0%, its viscosity assumes a value of 16.52 mPa·s, which is considered adequate for coal mine application; meanwhile, the anti-evaporation characteristic and the dust suppression efficiency of the dust suppressant solution both reach optimal level under this concentration. Therefore, based on a comprehensive comparative study covering the factors elaborated above, it is determined that the optimal concentration of the current SDS-SPI cementing dust suppressant solution is 3%.

4. Analysis of Dust Suppression Mechanism

4.1. Infrared Spectra Tests

The current experiment was tested using a Nicolet iS10 Fourier-Transform infrared spectrometer (Beijing Kaifeng Fengyuan Technology Co., Ltd., Beijing, China). First, the sample was mixed with potassium bromide in an agate mortar at a ratio of 1:200. The ground mixture powder was then made into transparent thin pellets for testing. The test measurement range is between 4000 and 500 cm^{-1}, and each sample is scanned 6 times. The infrared spectrum before and after SPI modification is shown in Figure 9, where (A) is the spectrum of SPI, and (B) is the corresponding spectra after SPI modification.

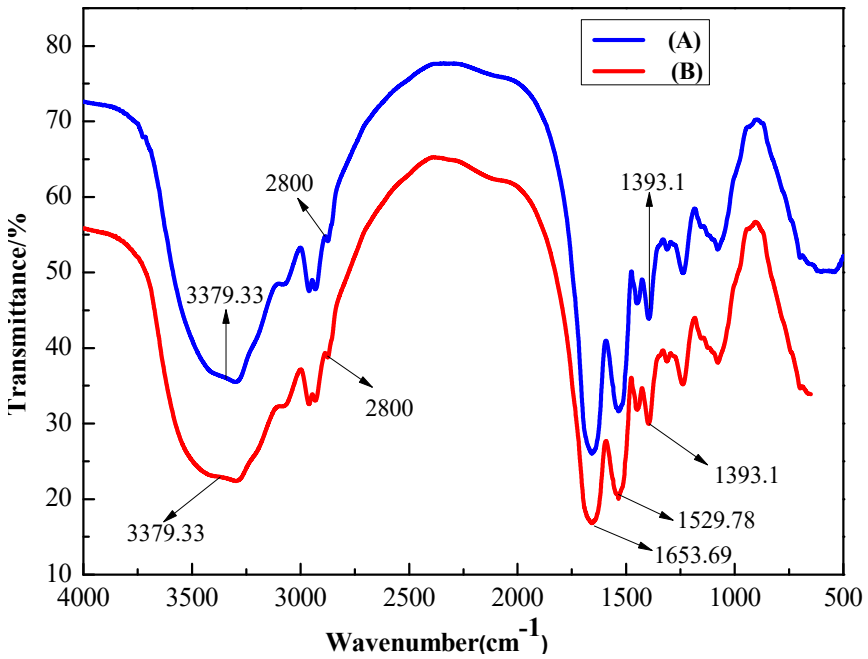

Figure 9. The infrared spectra of SPI before and after the SDS modification.

Figure 9 shows the infrared spectra of SPI before and after SDS modification. As can be seen from the figure, the wave number of 3379.33 cm^{-1} mainly corresponds to the spectral peaks of –NH, –OH and sulfonamide bond; The wave number 2800 cm^{-1} corresponds to the absorption peak of CH_2. Wave number 1653.69 cm^{-1} corresponds to C=O stretching peak in band I of amide; The wave number of 1529.78 cm^{-1} corresponds to the superposition peaks of N–H bending vibration and C–N stretching vibration in band II, as well as the absorption peaks of sulfa bonds. The wave number of 1393.1 cm^{-1} corresponds to the characteristic peaks of sulfa bond and COO–. The wave numbers of these two peaks are 1653.69 cm^{-1} and 1529.78 cm^{-1} respectively, which correspond to the characteristic spectral peaks and their bending vibration of the benzene ring in the C–H [70–75].

After modification, the spectral peaks at 3379.33 cm^{-1} and 1393.1 cm^{-1} in Figure 9B (representing the sulfonamide bond) moved to the left with a slight increase in amplitude, indicating that the addition of anionic surfactant SDS in the modification of SPI with anionic surfactant SDS would destroy the dense structure existing in SPI and relax SPI. This process may result in the formation of protein-surfactant (SDS-SPI) complex chemicals. In addition, loose connections between domains are compromised, resulting in a decrease in the molecular weight of the protein, which can be enhanced if it occurs within a certain range [76–82]. At the same time, comparing the results before and after the modification, it was found that the modified SDS-SPI moved to the left at the absorption peaks of 3377.33 cm^{-1}, 2800 cm^{-1} and 1393.1 cm^{-1} during the strengthening process. This indicates that the amount of newly formed SDS-SPI composite chemicals increases, leading to an increase in the relaxation degree of SPI structure. At the same time, the internal hydrophobic functional group is transformed outward, which improves the water solubility of SPI. The more relaxed the protein structure, the more functional groups, the better the coal dust cementing effect. Although the peaks of 1653.69 cm^{-1} and 1529.78 cm^{-1} were basically stable, the intensity increased slightly, indicating that the benzene ring entered the SPI molecular structure, further confirming the formation of SDS-SPI complex chemistry. At the same time, under the influence of SDS, a group of different hydrophilic functional groups move inward and the hydrophobicity is enhanced. CMC is a commonly used viscosifier that enhances the viscosifying effect of the anionic surfactant SDS. Methanesiliconic acid sodium is a water-resistant enhancer that interacts with CO_2 in the air to cause polycondensation between molecules to form a macromolecular structure that is spatially interconnected. The hydrophilic

hydroxyl group in the polycondensation process is converted into a hydrophobic Si–O bond, so that the reagent has strong water resistance.

4.2. Scanning Electron Microscope (SEM) Experiments

The current experiment employs D-type high-resolution SEM to investigate the surface morphology of the sample. Three sets of samples are selected, and the coal powder used here is coking coal derived from the 20206 mechanized mining face of Shandong Zaozhuang Corporation's Jiangzhuang Coal Mine. A planetary motion micro mill is used to grind the coal chunks into fine powder for the tests. Figure 10 shows the 5000× SEM image of dry coal powder; Figure 11 shows the 5000× SEM photo of coal powder treated with SPI only; Figure 12 shows the 5000× SEM photo of coal powder treated by the developed SDS-SPI cementing dust suppressant solution with optimal spray concentration.

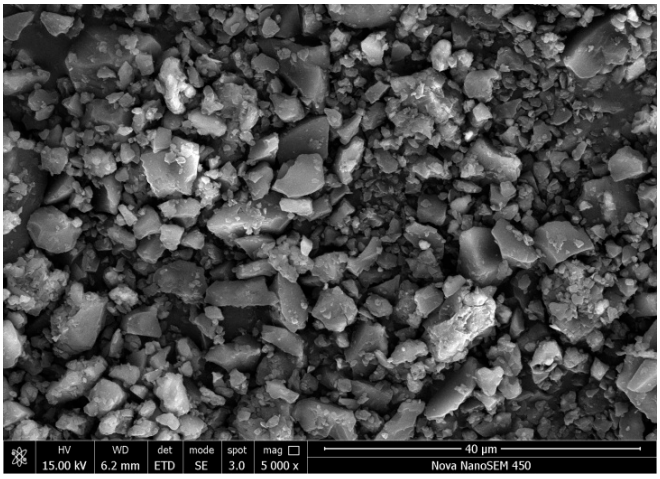

Figure 10. 5000× SEM image of dry coal powder.

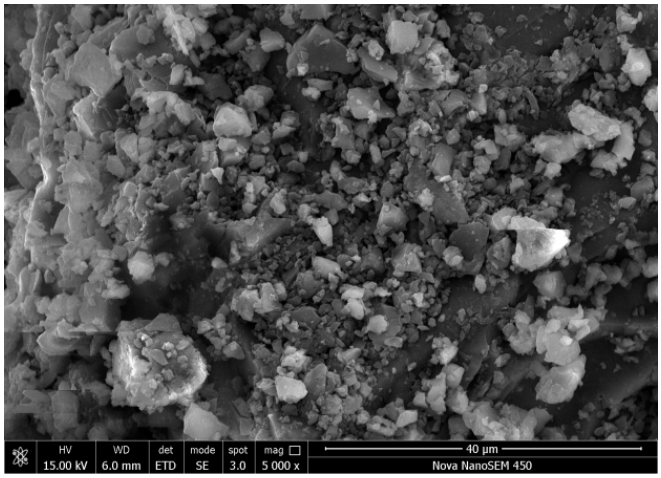

Figure 11. SEM photo of coal powder treated with SPI.

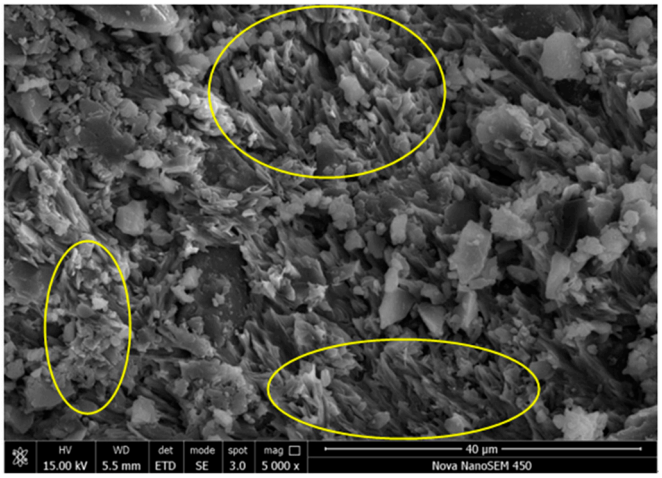

Figure 12. 5000× SEM image of coal powder treated by the developed SDS-SPI cementing dust suppressant solution with optimal spray concentration.

In order to study the effect of dust suppressant on the cementation hardening effect of pulverized coal before and after modification, three groups of pulverized coal were scanned by SEM in this study. The surface morphology is shown in Figures 10–12. Figure 10 is a 5000× SEM image of the surface morphology of the dry powder. Under this circumstance, it was found that the shape and size of the coal dust particles changed greatly, the particle spacing was large, and there was a lack of cementation between the particles. In this case, the coal powder is highly susceptible to the dispersion of air, causing dust pollution. Figure 11 shows the SEM pulverized coal 5000× SEM image. The study found that the coal dust particles are tightly bonded and the cementation spacing is small. This is mainly driven by the viscosity of the SPI. Figure 12 is a 5000× SEM image of pulverized coal treated with the optimal concentration of the developed SDS-SPI cementing dust suppression solution. It can be seen from the yellow circle area in the figure that the coal powder particles are tightly cemented, the cementation strength is high, and the cementation spacing between the coal powder particles is small. This indicates that the viscosity of the SDS-SPI compound chemical modification is increased, which is consistent with the viscosity test results of this study; the SDS-SPI cementing dust suppression solution modified by SPI can form a dense layer on the surface of the coal powder. The hardened shell layer cements pulverized coal particles of different particle sizes, and the cementing effect is good, thereby suppressing the re-flying of coal dust.

5. Conclusions

(1) The newly developed environmentally-friendly dust suppressant uses SPI as the main cementing ingredient, carboxymethylcellulose sodium as the viscosity enhancer, and methanesiliconic acid sodium as the water resisting additive. Based on modifying SPI with anionic surfactant sodium dodecyl sulfonate, a novel biodegradable environmentally-friendly cementing dust suppressant is prepared.

(2) It is best to use anionic surfactant (SDS) to modify SPI so as to destroy and relax its original compact sphere structure, forming protein-surfactant (SDS-SPI) composite chemical. After the modification, the hydrophobic functional groups inside the protein-surfactant composite chemical move outward, allowing the coal dust to better absorb the hydrophobic functional groups such that the coal dust is more thoroughly cemented for delivering the dust suppression effect.

(3) Compared to SPI solution, the modification further improves the viscosity and water retention of the SDS-SPI cementing dust suppressant solution; based on a comprehensive comparison concerning water retention, viscosity and dust suppression efficiency of dust suppressant, the optimal concentration of dust suppressant solution is finally determined to be 3%. At this level, the

anti-evaporation and water retention characteristics are optimal, with the dust suppression effect being maximized.

(4) The present study conducts SEM high-resolution scanning over the surfaces of native coal powder, coal powder with SPI, and coal powder with dust suppressant at optimal concentration. At 5000×, it is found that the coal powder particles are compactly cemented when the dust suppressant at optimal concentration is applied, exhibiting a strong cementing power. Also, a layer of compact hardened shell forms at the surface, leading to a decent dust suppression effect.

(5) SPI, as the main material used in the present experiment, contains a large number of functional groups, which has an array of favorable properties, including being naturally occurring and being biodegradable. This further demonstrates that the independently developed dust suppressant is biodegradable, environmentally-friendly and clean, and does not pose any threat to the environment.

Author Contributions: H.J. and W.N. conceived and designed the experiments; H.J. and Y.Z. performed the experiments; J.Y. and H.Z. analyzed the data; H.W. contributed materials; H.J. and Q.B. wrote the paper; H.J. and W.N. revised the manuscript.

Funding: The research was financially supported by the National Natural Science Foundation of China (NO. 51874191 and 51404147), the Focus on Research and Development Plan in Shandong Province (NO.2017GSF20111), the National Key R&D Program of China (2017YFC0805201), the China Postdoctoral Science Foundation (NO. 2015M570601 and 2017T100503), the Open Foundation for Key Laboratory of Mine Disaster Prevention and Control in Hebei Province (KJZH2017K09).

Acknowledgments: This work has been funded by the China Postdoctoral Science Foundation (NO. 2015M570601 and 2017T100503), the National Natural Science Foundation of China (NO. 51874191 and 51404147), the Focus on Research and Development Plan in Shandong Province (NO. 2017GSF20111), the National Key R&D Program of China (2017YFC0805201).

Conflicts of Interest: The authors declare no conflict of interest.

References

1. Hattori, T.; Matsuda, M.; Miyake, M. Resource recovery of cupola dust: Study on sorptive property and mechanism for hydrogen sulfide. *J. Mater. Sci.* **2006**, *12*, 3701–3706. [CrossRef]
2. Wang, Y.X.; Guo, P.P.; Dai, F.; Li, X.; Zhao, Y.L.; Liu, Y. Behavior and modeling of fiber-reinforced clay under triaxial compression by combining the superposition method with the energy-based homogenization technique. *Int. J. Geomech.* **2018**, *18*. [CrossRef]
3. Cheng, W.M.; Nie, W.; Zhou, G.; Yu, Y.B.; Ma, Y.Y.; Xue, J. Research and practice on fluctuation water injection technology at low permeability coal seam. *Saf. Sci.* **2012**, *50*, 851–856. [CrossRef]
4. Cai, P.; Nie, W.; Chen, D.W.; Yang, S.B.; Liu, Z.Q. Effect of air flowrate on pollutant dispersion pattern of coal dust particles at fully mechanized mining face based on numerical simulation. *Fuel* **2019**, *239*, 623–635. [CrossRef]
5. Wang, Y.X.; Guo, P.P.; Li, X.; Lin, H.; Liu, Y.; Yuan, H.P. Behavior of Fiber-Reinforced and Lime-Stabilized Clayey Soil in Triaxial Tests. *Appl. Sci.* **2019**, *9*, 900. [CrossRef]
6. Peng, X.L.; Wu, C. New advances in chemical dust suppressants. *J. Saf. Sci. Technol.* **2005**, *5*, 44–47.
7. Cai, J.X.; Dong, B.; Li, Y.Q. New Experimental Research dust suppressants in Bulk coal yard Applicability. *Mine Environ. Prot.* **2011**, *21*, 71–73.
8. Wang, Y.X.; Guo, P.P.; Ren, W.X.; Yuan, B.X.; Yuan, H.P.; Zhao, Y.L.; Shan, S.B.; Cao, P. Laboratory investigation on strength characteristics of expansive soil treated with jute fiber reinforcement. *Int. J. Geomech.* **2017**, *17*. [CrossRef]
9. Yang, S.B.; Nie, W.; Liu, Z.Q.; Peng, H.T.; Cai, P. Effects of spraying pressure and installation angle of nozzles on atomization characteristics of external spraying system at a fully-mechanized mining face. *Powder Technol.* **2019**, *343*, 754–764. [CrossRef]
10. Yuan, B.X.; Sun, M.; Wang, Y.X.; Zhai, L.H.; Luo, Q.; Zhang, X. Full 3D displacement measuring system for 3D displacement field of soil around a laterally loaded pile in transparent soil. *Int. J. Geomech.* **2019**, *19*, 04019028. [CrossRef]

11. Zhang, H.H.; Nie, W.; Liu, Y.H.; Wang, H.K.; Jin, H.; Bao, Q. Synthesis and performance measurement of environment-friendly solidified dust suppressant for open pit coalmine. *J. Appl. Polym. Sci.* **2018**, *135*, 46505. [CrossRef]
12. Nie, W.; Ma, X.; Cheng, W.M.; Liu, Y.H.; Xin, L.; Peng, H.T.; Wei, W.L. A novel spraying/negative-pressure secondary dust suppression device used in fully mechanized mining face: A case study. *Saf. Environ.* **2016**, *103*, 126–135. [CrossRef]
13. Cheng, W.M.; Liu, W.; Nie, W.; Zhou, G.; Cui, X.F.; Sun, X. The Prevention and Control Technology of Dusts in Heading and Winning Faces and Its Development Tendency. *J. Shandong Univ. Sci. Technol. (Nat. Sci.)* **2010**, *4*, 77–82.
14. Cai, P.; Nie, W.; Hua, Y.; Wei, W.L.; Jin, H. Diffusion and pollution of multi-source dusts in a fully mechanized coal face. *Process. Saf. Environ.* **2018**, *118*, 93–105. [CrossRef]
15. Liu, L.; Fang, Z.Y.; Qi, C.C.; Zhang, B.; Guo, L.J.; Song, K.-I. Numerical study on the pipe flow characteristics of the cemented paste backfill slurry considering hydration effects. *Powder Technol.* **2019**, *343*, 454–464. [CrossRef]
16. Wang, M.; Liu, L.; Zhang, X.Y.; Liu, C.; Wang, S.Q.; Jia, Y.H. Experimental and numerical investigations of heat transfer and phase change characteristics of cemented paste backfill with PCM. *Appl. Therm. Eng.* **2019**, *150*, 121–131. [CrossRef]
17. Liu, X.S.; Tan, Y.L.; Ning, J.G.; Lu, Y.W.; Gu, Q.H. Mechanical properties and damage constitutive model of coal in coal-rock combined body. *Int. J. Rock Mech. Min.* **2018**, *110*, 140–150. [CrossRef]
18. Wang, H.T.; Wang, D.M.; Wang, Q.G.; Jia, Z.Q. Novel Approach for Suppressing Cutting Dust Using Foam on a Fully Mechanized Face with Hard Parting. *J. Occup. Environ. Hyg.* **2013**, *3*, 154–164. [CrossRef] [PubMed]
19. Hu, S.Y.; Feng, R.; Ren, X.Y.; Xu, G.; Chang, P.; Wang, Z.; Zhang, Y.T.; Li, Z.; Gao, Q. Numerical study of gas-solid two-phase flow in a coal roadway after blasting. *Adv. Powder Technol.* **2016**, *4*, 1607–1617. [CrossRef]
20. Wang, H.T.; Wang, D.M.; Ren, W.X.; Lu, X.; Han, F.W.; Zhang, Y.K. Application of foam to suppress rock dust in a large cross-section rock roadway driven with roadheader. *Adv. Powder Technol.* **2012**, *1*, 257–262. [CrossRef]
21. Hu, S.Y.; Wang, Z.; Feng, G.R. Temporal and Spatial Distribution of Respirable Dust After Blasting of Coal Roadway Driving Faces: A Case Study. *Minerals* **2015**, *4*, 679–692. [CrossRef]
22. Wang, H.; Nie, W.; Cheng, W.M.; Liu, Q.; Jin, H. Effects of air volume ratio parameters on air curtain dust suppression in a rock tunnel's fully-mechanized working face. *Adv. Powder Technol.* **2018**, *29*, 230–244. [CrossRef]
23. Wang, Y.X.; Guo, P.P.; Lin, H.; Li, X.; Zhao, Y.L.; Yuan, B.X.; Liu, Y.; Cao, P. Numerical Analysis of Fiber-Reinforced Soils based on the Equivalent Additional Stress Concept. *Int. J. Geomech.* **2019**, in press.
24. Liu, Q.; Nie, W.; Hua, Y.; Peng, H.T.; Liu, C.Q.; Wei, C.H. Research on tunnel ventilation systems: Dust diffusion and pollution behaviour by air curtains based on CFD technology and field measurement. *Build. Environ.* **2019**, *147*, 444–460. [CrossRef]
25. Wang, Q.G.; Wang, D.M.; Wang, H.T.; Han, F.W.; Zhu, X.L.; Tang, Y.; Si, W.B. Optimization and implementation of a foam system to suppress dust in coal mine excavation face. *Process Saf. Environ.* **2015**, *96*, 184–190. [CrossRef]
26. Han, F.W.; Liu, J. Flow field characteristics and coal dust removal performance of an arc fan nozzle used for water spray. *PLoS ONE* **2018**, *13*, 0203875. [CrossRef] [PubMed]
27. Wang, Z.; Gao, W.; Zhang, P.; Yan, H.J.; Ren, C.S. Study of the Characteristics of DC and ICP Hybrid Discharge Plasmas. *Plasma Sci. Technol.* **2015**, *3*, 191–195. [CrossRef]
28. Lyu, X.J.; You, X.F.; He, M.; Zhang, W.; Wei, H.B.; Li, L.; He, Q. Adsorption and molecular dynamics simulations of nonionic surfactant on the low rank coal surface. *Fuel* **2018**, *211*, 529–534. [CrossRef]
29. Liu, L.; Fang, Z.Y.; Wu, Y.P.; Lai, X.P.; Wang, P.; Song, K.-I. Experimental investigation of solid-liquid two-phase flow in cemented rock-tailings backfill using Electrical Resistance Tomography. *Constr. Build. Mater.* **2018**, *175*, 267–276. [CrossRef]
30. Nie, W.; Peng, H.T.; Jin, H.; Liu, Y.H.; Wei, W.L. The effect of spray pressure on atomization characteristics of external spray nozzle on coal mining machine. *J. Chin. Univ. Min. Technol.* **2017**, *46*, 41–47.
31. Wang, H.T.; He, S.; Xie, G.R.; Chen, X.Y.; Qin, B.T. Study of the mechanism by which magnetization reduces dust suppressant usage. *Colloids Surf. A* **2018**, *558*, 16–22. [CrossRef]

32. Liu, Y.H.; Nie, W.; Jin, H.; Ma, H.; Hua, Y.; Cai, P.; Wei, W.L. Solidifying dust suppressant based on modified chitosan and experimental study on its dust suppression performance. *Adsorpt. Sci. Technol.* **2018**, *36*, 640–654. [CrossRef]
33. Yuan, Q.H.; Xu, X.J.; Liu, Q.; Zhang, X.J. Medium Consumption Control in Dense Medium Coal Preparation Plant Based on Response Surface Methodology. *J. Shandong Univ. Sci. Technol. (Nat. Sci.)* **2018**, *37*, 11–21. [CrossRef]
34. Kong, B.; Li, Z.H.; Wang, E.Y.; Liu, W.; Chen, L.; Qi, G.S. An experimental study for characterization the process of coal oxidation and spontaneous combustion by electromagnetic radiation technique. *Process Saf. Environ.* **2018**, *119*, 285–294. [CrossRef]
35. Ding, Y.M.; Ezekoye, O.A.; Zhang, J.Q.; Wang, C.J.; Lu, S.X. The effect of chemical reaction kinetic parameters on the bench-scale pyrolysis of lignocellulosic biomass. *Fuel* **2018**, *232*, 147–153. [CrossRef]
36. Cheng, W.M.; Liu, Z.; Yang, H.; Wang, W.Y. Non-linear Seepage Characteristics and Influential Factors of Water Injection in Gassy Seams. *Exp. Therm. Fluid Sci.* **2018**, *91*, 41–53. [CrossRef]
37. Yang, J.; Liu, D.D.; Zhu, X.L.; Fang, X.M. Research progress of chemical dust suppression agent. *Chemistry* **2013**, *4*, 346–353.
38. Sa, Z.Y.; Liu, J.; Liu, J.Z.; Zhang, Y.J. Research on effect of gas pressure in the development process of gassy coal extrusion. *Saf. Sci.* **2019**, *115*, 28–35. [CrossRef]
39. Liu, Y.; Wang, M.Y.; Zhao, S.S.; Liu, Y.Y.; Yang, J. Synthesis and Modification of Hyperbranched Polyester Dust Suppressant. *J. Shandong Univ. Sci. Technol. (Nat. Sci.)* **2018**, *37*, 26–34. [CrossRef]
40. Nie, W.; Peng, H.T.; Liu, Y.H.; Ma, X.; Wei, W.L. Experimental Research on the Coupling and Settlement of Droplets and Dust Particles Influenced by Airflow. *J. Shandong Univ. Sci. Technol. (Nat. Sci.)* **2016**, *35*, 30–36. [CrossRef]
41. Kong, B.; Wang, E.Y.; Li, Z.H. The effect of high temperature environment on rock properties—An example of electromagnetic radiation characterization. *Environ. Sci. Pollut. R.* **2018**, *25*, 29104–29114. [CrossRef] [PubMed]
42. Liu, Z.; Yang, H.; Wang, W.Y.; Cheng, W.M.; Xin, L. Experimental Study on the Pore Structure Fractals and Seepage Characteristics of a Coal Sample Around a Borehole in Coal Seam Water Infusion. *Transp. Porous Med.* **2018**, *125*, 289–309. [CrossRef]
43. Bao, Q.; Nie, W.; Liu, C.Q.; Liu, Y.H.; Zhang, H.H.; Wang, H.K.; Jin, H. Preparation and characterization of a binary-graft-based, water-absorbing dust suppressant for coal transportation. *J. Appl. Polym. Sci.* **2018**, *136*, 47065. [CrossRef]
44. Grogan, R. Mixtures, Compositions, and Methods of Using and Preparing Same. Patent US 20090269499, 29 October 2009.
45. Zhang, L.B.; Jiao, J.; Zhao, X.Y.; Zhang, J.; Zou, D.; Ji, Y.; Shan, C. Study on preparation and properties of eco-friendly dust suppressant. *Trans. Chin. Soc. Agric. Eng.* **2013**, *18*, 218–225.
46. Zhang, H.H.; Nie, W.; Wang, H.K.; Bao, Q.; Jin, H.; Liu, Y.H. Preparation and experimental dust suppression performance characterization of a novel guar gum-modification-based environmentally-friendly degradable dust suppressant. *Powder Technol.* **2018**, *339*, 314–325. [CrossRef]
47. Yang, J.; Wang, K.; Fang, X.M. The Preparation and Performance Test of a New Coal Dust Depressor. *Saf. Coal Mines* **2009**, *5*, 21–24.
48. Polat, H.; Chander, S. Adsorption of PEO/PPO Triblock Co-polymers and Wetting of Coal. *Colloids Surf. A Physicochem. Eng. Asp.* **1999**, *1*, 199–212. [CrossRef]
49. Zhou, Q.; Qin, B.T.; Wang, J.; Wang, H.T.; Wang, F. Experimental investigation on the changes of the wettability and surface characteristics of coal dust with different fractal dimensions. *Colloids Surf. A* **2018**, *551*, 148–157. [CrossRef]
50. Liu, Q.; Nie, W.; Hua, Y.; Peng, H.T.; Liu, Z.Q. The effects of the installation position of a multi-radial swirling air-curtain generator on dust diffusion and pollution rules in a fully-mechanized excavation face: A case study. *Powder Technol.* **2018**, *329*, 371–385. [CrossRef]
51. Liu, Y.H.; Nie, W.; Mu, Y.B.; Zhang, H.H.; Wang, H.K.; Jin, H.; Liu, Z.Q. A synthesis and performance evaluation of a highly efficient ecological dust depressor based on the sodium lignosulfonate–acrylic acid graft copolymer. *RSC Adv.* **2018**, *8*, 11498–11508. [CrossRef]

52. Zhao, Y.L.; Zhang, L.Y.; Wang, W.J.; Wan, W.; Li, S.Q.; Ma, W.H.; Wang, Y.X. Creep behavior of intact and cracked limestone under multi-level loading and unloading cycles. *Rock Mech. Rock Eng.* **2017**, *50*, 1409–1424. [CrossRef]
53. Liu, L.; Fang, Z.Y.; Qi, C.C.; Zhang, B.; Guo, L.J.; Song, K.-I. Experimental investigation on the relationship between pore characteristics and unconfined compressive strength of cemented paste backfill. *Constr. Build. Mater.* **2018**, *179*, 254–264. [CrossRef]
54. Qin, B.T.; Dou, G.L.; Zhong, X.X. Effect of stannous chloride on low-temperature oxidation reaction of coal. *Fuel Process. Technol.* **2018**, *176*, 59–63. [CrossRef]
55. Li, L.; Qin, B.T.; Ma, D.; Zhuo, H.; Liang, H.J.; Gao, A. Unique spatial methane distribution caused by spontaneous coal combustion in coal mine goafs: An experimental study. *Process Saf. Environ.* **2018**, *116*, 199–207. [CrossRef]
56. Zhao, Y.J.; Li, R.Y.; Ji, C.F.; Huan, C.; Zhang, B.; Liu, L. Parametric study and design of an earth air heat exchanger using model experiment for memorial heating and cooling. *Appl. Therm. Eng.* **2019**, *148*, 838–845. [CrossRef]
57. Liu, X.S.; Gu, Q.H.; Tan, Y.L.; Ning, J.G.; Jia, Z.C. Mechanical Characteristics and Failure Prediction of Cement Mortar with a Sandwich Structure. *Minerals* **2019**, *9*, 143. [CrossRef]
58. Nie, W.; Liu, Y.H.; Wang, H.; Wei, W.L.; Peng, H.T.; Cai, P.; Hua, Y.; Jin, H. The development and testing of a novel external-spraying injection dedusting device for the heading machine in a fully-mechanized excavation face. *Process Saf. Environ.* **2017**, *109*, 716–731. [CrossRef]
59. Nie, W.; Wei, W.L.; Ma, X.; Liu, Y.H.; Peng, H.T.; Liu, Q. The effects of ventilation parameters on the migration behaviors of head-on dusts in the heading face. *Tunn. Undergr. Space Technol.* **2017**, *70*, 400–408. [CrossRef]
60. Hua, Y.; Nie, W.; Wei, W.L.; Liu, Q.; Liu, Y.H.; Peng, H.T. Research on multi-radial swirling flow for optimal control of dust dispersion and pollution at a fully mechanized tunnelling face. *Tunn. Undergr. Space Technol.* **2018**, *79*, 293–303. [CrossRef]
61. Dimech, C.C.; Cheeseman, R.; Cook, S.; Simon, J.; Boccaccini, A.R. Production of sintered materials from air pollution control residues from waste incineration. *J. Mater. Sci.* **2008**, *12*, 4143–4151. [CrossRef]
62. Li, T.Y.; Wang, N.; Fang, Q.H. Incorporation of modified soy protein isolate as filier in BR/SBR blends. *J. Mater. Sci.* **2010**, *7*, 1904–1911. [CrossRef]
63. Zhong, X.X.; Qin, B.T.; Dou, G.L.; Xia, C.; Wang, F. A chelated calcium-procyanidine-attapulgite composite inhibitor for the suppression of coal oxidation. *Fuel* **2017**, *217*, 680–688. [CrossRef]
64. Nie, W.; Wei, W.L.; Cai, P.; Liu, Z.Q.; Liu, Q.; Ma, H.; Liu, H.J. Simulation experiments on the controllability of dust diffusion by means of multi-radial vortex airflow. *Adv. Powder Technol.* **2018**, *29*, 835–847. [CrossRef]
65. Wang, Y.X.; Lin, H.; Zhao, Y.L.; Li, X.; Guo, P.P.; Liu, Y. Analysis of fracturing characteristics of unconfined rock plate under edge on impact loading. *Eur. J. Environ Civ. Eng.* **2019**. [CrossRef]
66. Peng, H.T.; Nie, W.; Cai, P.; Liu, Q.; Liu, Z.Q.; Yang, S.B. Development of a novel wind-assisted centralized spraying dedusting device for dust suppression in a fully mechanized mining face. *Environ. Sci. Pollut. Res.* **2018**. [CrossRef] [PubMed]
67. Chen, D.W.; Nie, W.; Cai, P.; Liu, Z.Q. The diffusion of dust in a fully-mechanized mining face with a mining height of 7 m and the application of wet dust-collecting nets. *J. Clean. Prod.* **2018**, *205*, 463–476. [CrossRef]
68. Zhao, Y.L.; Luo, S.L.; Wang, Y.X.; Wang, W.J.; Zhang, L.Y.; Wan, W. Numerical Analysis of Karst Water Inrush and a Criterion for Establishing the Width of Water-resistant Rock Pillars. *Mine Water Environ.* **2017**, *36*, 508–519. [CrossRef]
69. Liu, L.; Zhu, C.; Qi, C.C.; Zhang, B.; Song, K.-I. A microstructural hydration model for cemented paste backfill considering internal sulfate attacks. *Constr. Build. Mater.* **2019**, in press.
70. Kim, J.R.; Netravali, A.N. Parametric study of protein-encapsulated microcapsule formation and effect on self-healing efficiency of 'green' soy protein resin. *J. Mater. Sci.* **2017**, *6*, 3028–3047. [CrossRef]
71. Jin, H.; Nie, W.; Zhang, H.H.; Liu, Y.H.; Bao, Q.; Wang, H.K. The Preparation and Characterization of a Novel Environmentally-Friendly Coal Dust Suppressant. *J. Appl. Polym. Sci.* **2018**, *136*, 47354. [CrossRef]
72. Liu, C.Q.; Nie, W.; Bao, Q.; Liu, Q.; Wei, C.H.; Hua, Y. The effects of the pressure outlet's position on the diffusion and pollution of dust in tunnel using a shield tunneling machine. *Energy Build.* **2018**, *176*, 232–245. [CrossRef]

73. Zhao, Y.L.; Tang, J.Z.; Chen, Y.; Zhang, L.Y.; Wang, W.J.; Liao, J.P. Hydromechanical coupling tests for mechanical and permeability characteristics of fractured limestone in complete stress–strain process. *Environ. Earth Sci.* **2017**, *76*, 1–18. [CrossRef]
74. Zhao, Y.J.; Zhang, Z.H.; Ji, C.F.; Liu, L.; Zhang, B.; Huan, C. Characterization of particulate matter from heating and cooling several edible oils. *Build. Environ.* **2019**, *152*, 204–213. [CrossRef]
75. Ding, Y.M.; Zhou, R.; Wang, C.J.; Lu, K.H.; Lu, S.X. Modeling and analysis of bench-scale pyrolysis of lignocellulosic biomass based on merge thickness. *Bioresour. Technol.* **2018**, *268*, 77–80. [CrossRef] [PubMed]
76. Luo, R.D.; Lin, M.S.; Luo, Y.B.; Dong, J.F. Preparation and properties of a new type of coal dust suppressant. *J. Chin. Coal Soc.* **2016**, *41*, 454. [CrossRef]
77. Wei, Q.H.; Tong, L.; Chen, N.L.; Lin, Q.J. Adhesive properties of a soy-based wood adhesive using sodium dodecyl sulfate. *J. Zhejiang For. Coll.* **2008**, *6*, 772–776.
78. Hua, Y.; Nie, W.; Cai, P.; Liu, Y.H.; Peng, H.T.; Liu, Q. Pattern characterization concerning spatial and temporal evolution of dust pollution associated with two typical ventilation methods at fully mechanized excavation faces in rock tunnels. *Powder Technol.* **2018**, *334*, 117–131. [CrossRef]
79. Zhao, Y.L.; Wang, Y.X.; Wang, W.; Tang, L.; Liu, Q.; Cheng, G. Modeling of rheological fracture behavior of rock cracks subjected to hydraulic pressure and far field stresses. *Theor. Appl. Fract. Mech.* **2019**. [CrossRef]
80. Qi, C.C.; Chen, Q.S.; Fourie, A.; Tang, X.L.; Zhang, Q.L.; Dong, X.J.; Feng, Y. Constitutive modelling of cemented paste backfill: A data-mining approach. *Constr. Build. Mater.* **2019**, *197*, 262–270. [CrossRef]
81. Liu, Z.Q.; Nie, W.; Peng, H.T.; Yang, S.B.; Chen, D.W.; Liu, Q. The effects of the spraying pressure and nozzle orifice diameter on the atomizing rules and dust suppression performances of an external spraying system in a fully-mechanized excavation face. *Powder Technol.* **2019**, in press. [CrossRef]
82. Liu, J.; Zhang, R.; Song, D.Z.; Wang, Z.Q. Experimental investigation on occurrence of gassy coal extrusion in coalmine. *Saf. Sci.* **2019**, *113*, 362–371. [CrossRef]